Cirrus parametrization and the role of ice nuclei

By C. REN* and A. R. MACKENZIE

Environment Science Department, Lancaster University, UK

SUMMARY

A parametrization of cirrus clouds formed by homogeneous nucleation is improved so that it can be used more easily in general-circulation models (GCMs) and climate models. The improved parametrization is completely analytical and requires no fitting of parameters to models or measurements; it compares well with full microphysical model results even when monodisperse aerosol particles are used in the parametrization to determine cirrus ice-crystal number densities. However, the presence of ice nuclei in the atmosphere can modify the formation of cirrus clouds. If sufficient ice particles have been generated by heterogeneous nucleation, the saturation ratio of the air parcel will never reach that required for homogeneous nucleation. We calculate the critical number density of ice nuclei, above which homogeneous nucleation will be suppressed. The critical number density depends on the temperature, the updraught velocity, and the supersaturation at which ice nuclei activate. The theory points to key uncertainties in our observations of ice nuclei in the upper troposphere; for ice nuclei that activate at relatively low supersaturations, number density is more important than a precise knowledge of the activation supersaturation. Overall, the theory provides a general framework within which to interpret observations and the results of full microphysical cloud models. The theory can provide analytical test cases as benchmarks for the testing of models in development, and can be implemented itself into larger-scale atmospheric models, such as GCMs.

KEYWORDS: Aerosols   Heterogeneous nucleation   Homogeneous nucleation   Modelling

1. INTRODUCTION

The indirect effect of aerosol on radiation and climate is the most uncertain part in climate change (IPCC 2001). An example of this is the role of cirrus clouds in climate (Lynch 1996). The net radiative effect of their presence is the result of competition between the solar albedo and IR greenhouse effects, which is extremely sensitive to crystal shape and the crystal-size distribution (Zhang *et al.* 1999).

In a newly formed cirrus cloud, the most important parameter in the size distribution is the number density. Given the synoptic conditions, the water vapour available for deposition is approximately fixed; the sizes of ice crystals are then determined by the sharing of water vapour according to their surface areas. In the upper troposphere, ice crystals form through homogeneous nucleation, as well as heterogeneous nucleation, if ice nuclei are present. For homogeneous nucleation, Sassen and Benson (2000) gave a parametrization based on numerical-model results that is only valid in the range of temperatures from -36 to $-60\,^{\circ}$C, and for updraughts from 0.04 to 1.0 m s^{-1}. Considering the competition between generating supersaturation by updraught and cooling and removing supersaturation by depositional growth of the ice crystals, Kärcher and Lohmann (2002a,b) calculated the number density of ice crystals at the peak value of supersaturation and achieved a parametrization for cirrus-cloud formation. Their parametrization uses a fitting parameter to match model results, and includes the complementary error function, which is not straightforward to use. For heterogeneous nucleation, most studies rely on empirical formulae, e.g. Lin *et al.* (2002). Kärcher and Lohmann (2003) extended their parametrization for homogeneous nucleation to heterogeneous immersion freezing by decreasing freezing thresholds. Care must be taken when making such an extension, because the surface area of solid particles (e.g. soot, DeMott *et al.* 1997) must be taken into account when determining the

---

* Corresponding author: Environment Science Department, Lancaster University, Lancaster LA1 4YQ, UK.
e-mail: c.ren@lancaster.ac.uk

nucleation rate. Gierens (2003) modelled the transition between heterogeneous and homogeneous cirrus formation, and yielded a critical value to mark the transition, which might be only valid for ice nuclei activating at supersaturations around 0.3. In this work, the number densities of ice crystals in cirrus clouds formed by aerosol freezing, both homogeneously and heterogeneously, in the upper troposphere are discussed using parametrized relationships. Nucleation regimes, either heterogeneous or homogeneous freezing, can be differentiated by comparing virtual supersaturation mixing ratios with the critical supersaturation mixing ratio required by homogeneous nucleation, as in section 2. The parametrization of homogeneous nucleation is improved by using a theoretically determined timescale of homogeneous freezing, and made practicable by providing a universal analytical expression, discussed in detail in section 3. The conditions for ice nuclei to suppress homogeneous nucleation are given in section 4, followed by a discussion of how a few existing ice crystals can depress secondary homogeneous nucleation, using a modelled test case. The summary and conclusions are given at the end. Symbols used in the text are defined in appendix B.

2. DIFFERENTIATING THE NUCLEATION REGIMES

In this section, an equation describing the revolution of water-vapour saturation ratios is achieved first. The equation is solved for an imaginary case. Homogeneous nucleation takes place only when the saturation ratio reaches a critical value. By comparing the saturation ratios with the critical value, we defined various nucleation regimes.

Consider an air parcel, lifted adiabatically at speed w, containing ice nuclei at the number density of N, which nucleate at saturation S_0. For simplicity, S_0 is assumed constant, and all the ice nuclei are the same size, r_0. Within the air parcel, the water-vapour saturation ratio with respect to ice changes with time as

$$\frac{dS}{dt} = \frac{d}{dt}\left(\frac{e}{e_{s,i}}\right) = \frac{1}{e_{s,i}}\frac{de}{dt} - S\frac{d\ln e_{s,i}}{dt}. \tag{1}$$

The water vapour pressure, e, changes through two processes, the deposition/sublimation process and the expansion that changes the partial pressure without changing the mixing ratio, i.e.

$$\frac{de}{dt} = -\frac{e - e_{s,i}}{\tau_g(t)} + \frac{e}{p}\frac{dp}{dt}, \tag{2}$$

where

$$\tau_g^{-1}(t) = 4\pi N D r_i(t) \tag{3}$$

is a parameter (bearing the dimension of the inverse of time) determined by the diffusivity of water molecules in air, D, the radius of ice particles, $r_i(t)$, and the number density of ice particles, N. Please note that these ice particles formed on ice nuclei, and we have used an assumption that one ice nucleus activates to become one ice particle.

Using the Clausius–Clapeyron equation for the saturation vapour pressure of water over ice at temperature, T,

$$\frac{d\ln e_{s,i}}{dt} = \frac{d\ln e_{s,i}}{dT}\frac{dT}{dt} = \frac{L_s}{R_v T^2}\frac{dT}{dt}, \tag{4}$$

where L_s is latent heat of sublimation, R_v is the gas constant of water vapour.
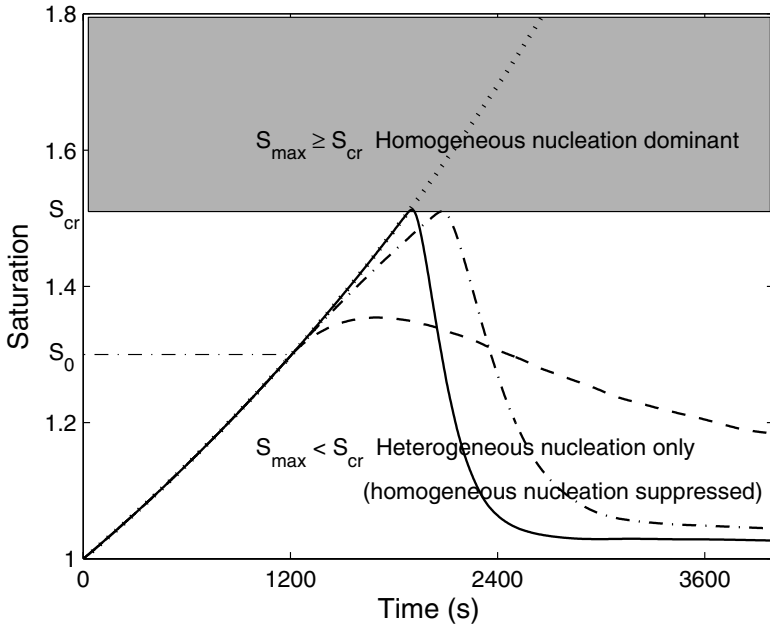
Figure 1. The change of saturation ratios with time for constantly ascending air parcels. The dotted line is for an imaginary case, showing the saturation ratio generated by a constant ascent; the solid line is for a case with no ice nuclei; the dash-dotted line is for a case with ice nuclei of 0.02 cm^{-3}; and the dashed line is for a case with ice nuclei of 0.1 cm^{-3}. Ice nuclei are assumed to activate at S_0 (see text).

Inserting (2) and (4) into (1), and introducing a thermodynamical timescale τ_u, we can achieve

$$\frac{\mathrm{d}S}{\mathrm{d}t} = \tau_u^{-1} S - \tau_g^{-1}(t)(S - 1), \tag{5}$$

where

$$\tau_u^{-1} = \frac{1}{p}\frac{\mathrm{d}p}{\mathrm{d}t} - \frac{L_s}{R_v T^2}\frac{\mathrm{d}T}{\mathrm{d}t} = a_1 w. \tag{6}$$

When the updraught is at constant speed w, with hydrostatic equilibrium assumption for p and adiabatic assumption for T, τ_u can be taken as a constant. a_1 is a coefficient given by Kärcher and Lohmann (2002a). However, because of the interaction between S and τ_g, there is no analytical solution to Eq. (5). Gierens (2003) has attempted to make one, but the significance of his solution is reduced by his having to prescribe τ_g as a known function of time, i.e. the growth rate of ice particles is known before the supersaturation is known. Alternatively, we can solve Eq. (5) numerically, by running a microphysical box model. Figure 1 shows examples of S evolution. The dotted line increases monotonically. This corresponds to an imaginary case, in which the depositional growth of ice particles doesn't consume water vapour. Mathematically, from Eq. (5) with $\tau_g = 0$, we have

$$\frac{\mathrm{d}S_u}{\mathrm{d}t} = \tau_u^{-1} S_u, \tag{7}$$

with initial condition

$$S_u(0) = S(0) = S_0, \tag{8}$$

where subscript 'u' denotes that we are considering the limit where only updraught controls the change of saturation ratio. In this case, we do have an analytical solution for the saturation ratio, i.e.

$$S_u(t) = S_0 \exp(t/\tau_u), \tag{9}$$

and S_u grows exponentially in an ascending air parcel. This imaginary case, although apparently trivial, is used later.

Except the dotted line, all other three lines are for real cases. The solid line is a case with no ice nuclei, the dash-dotted line is with ice nuclei of 0.02 cm^{-3}, the dashed line is with ice nuclei of 0.1 cm^{-3}. Because of homogeneous nucleation, the solid line and the dash-dotted line turn down just above a critical value of supersaturation. According to Sassen and Benson (2000), the turn requires a critical effective temperature at $\sim-38\,°C$, corresponding to a homogeneous nucleation rate coefficient of 10^{10} cm^{-3}s^{-1}. (The relationship between the rate coefficient and the homogeneous nucleation rate is given later by Eq. (16).) If this value of the homogeneous nucleation-rate coefficient is used to determine the critical value S_{cr}, its temperature dependence can be written as

$$S_{cr} = 2.349 - \frac{T}{259}, \tag{10}$$

with T in degrees absolute. This is an analytical fit to Koop *et al.*'s (2000) results, in contrast with numerical fittings by Kärcher and Lohmann (2002a) or Gierens (2003). The temperature in Eq. (10) is the ambient temperature, on the basis that Koop *et al.* (2000) assumed water droplets are in equilibrium with water vapour.

By comparing the saturation ratios $S(t)$ with S_{cr}, we can identify different nucleation regimes. When

$$S_{max} < S_{cr}, \tag{11}$$

the saturation is always below the value at which homogeneous nucleation takes place, and so the contribution of homogeneous nucleation to ice particles is negligible. We describe such a condition as a homogeneous-nucleation-suppressed case, which is discussed in section 4(a). When

$$S(t) \geq S_{cr}, \tag{12}$$

homogeneous nucleation does take place, and newly formed ice particles will soon start to produce a decrease of the saturation ratio with time, so that we can safely assume

$$S_{max} = S_{cr} \tag{13}$$

(see Fig. 1). If no ice crystals have nucleated on heterogeneous ice nuclei at saturation ratios below S_{cr}, then we have a pure-homogeneous-nucleation case, which is discussed in section 3. If some ice crystals have nucleated on heterogeneous ice nuclei, but saturation ratios at, or above, S_{cr} are reached, then we have a homogeneous-nucleation-dominant case, which is discussed in section 4(b).

3.   PURE HOMOGENEOUS NUCLEATION

It is believed that cirrus clouds not associated with convective clouds are often formed by homogeneous freezing of deliquescent aerosols in the upper troposphere (e.g. Santacesaria *et al.* 2003). Because of the radiative forcing of cirrus clouds, it is desirable to include those clouds in weather-forecasting and climate models. Kärcher and Lohmann (2002a,b) developed a cirrus parametrization for this purpose. Assuming ice particles are formed by homogeneous freezing of deliquescent aerosol droplets,

the parametrization determines the number density of ice particles by solving an equation governing the temporal evolution of saturation ratio over ice at its peak in a freezing event. At the peak of the saturation ratio, S, of an ascending air parcel,

$$\left.\frac{dS}{dt}\right|_{S \approx S_{cr}} = 0. \tag{14}$$

Resolving Eq. (14) can give the number density of ice particles formed by homogeneous freezing of a size-spectrum of droplets. We improve the parametrization as follows: (1) using a theoretically determined timescale of homogeneous nucleation, and (2) using a freezing/growth integral for monodisperse aqueous particles that has an analytic solution for all cases.

(a) On the nucleation timescale

The parametrization of cirrus clouds formed by homogeneous freezing follows the results of Ford (1998) and Koop *et al.* (2000). The expression given by Ford (1998) relates the nucleation rate some time before (at t_0), $\dot{n}_i(t_0)$, to the nucleation rate at present time t, $\dot{n}_i(t)$,

$$\dot{n}_i(t_0) = \dot{n}_i(t) \exp\left(-\frac{t - t_0}{\tau}\right). \tag{15}$$

Here the nucleation timescale, τ, is taken as a constant with respect to time. The nucleation timescale is in reverse proportion to the cooling rate. The following shows how this relationship is achieved by applying a result of Koop *et al.* (2000).

The homogeneous nucleation rate is proportional to the total volume of aqueous aerosols, V, with a homogeneous nucleation rate coefficient J,

$$\dot{n}_i(t) = J(t) \int_{r_s}^{\infty} \frac{4\pi}{3} r_0^3 \frac{dn_a}{dr_0}\, dr_0 = J(t) V(t), \tag{16}$$

where r_0 is the radius of aerosol particles, and n_a the number density of aerosol particles. Please note that n_a is a function of r_0 and t, and should be kept updated with t, i.e. the wet aerosol distribution at current supersaturation, instead of the initial/dry aerosol distribution.

By taking the logarithm of $\dot{n}_i(t)$ and differentiating it with respect to t from (15), we can get

$$\tau^{-1} = \frac{d \ln \dot{n}_i(t)}{dt}. \tag{17}$$

On substituting (16) into (17),

$$\tau^{-1} = \frac{d \ln J(t)}{dt} + \frac{d \ln V(t)}{dt}. \tag{18}$$

To relate τ to the cooling rate of the air parcel, we use the parametrization for J given by Koop *et al.* (2000), i.e.

$$J(t) = J\{\Delta a_w(t)\} = J\{\Delta a_w(T(t))\} = J\{T(t)\}, \tag{19}$$

where Δa_w is the excess of water activity, and T the temperature. By keeping the ambient water vapour pressure constant, as is the case before the ice deposition dominates the supersaturation change (neglecting the effect of atmospheric pressure change),

we achieve

$$\frac{\mathrm{d}\ln J(t)}{\mathrm{d}t} = \frac{\mathrm{d}\ln J(T)}{\mathrm{d}T}\frac{\mathrm{d}T(t)}{\mathrm{d}t} = C\frac{\mathrm{d}T}{\mathrm{d}t}, \tag{20}$$

where

$$C = -0.004T^2 + 2T - 304.4, \tag{21}$$

which is a simplified expression of $\mathrm{d}(\ln J)/\mathrm{d}T$, with errors less than 0.4%, when $\Delta a_{\mathrm{w}} = 0.3063$ (or $J = J_{\mathrm{cr}} = 10^{10}$ cm^{-3}s^{-1}) is used as a principal value for the formation of ice particles. The slight dependence of C on temperature, and hence on time, means that the assumption made by Ford (1998) is physically sound when the total volume of aqueous aerosols, $V(t)$, in (16) (and so in (18) as well) can be taken as constant during the nucleation event. So, a more physically sound C replaces the numerically fitted $c|\partial(\ln J)/\partial T|_{S=S_{\mathrm{cr}}}$ of Kärcher and Lohmann (2002a,b) to give an estimate of the nucleation timescale. The relationship we achieve here is

$$\tau^{-1} = C\frac{\mathrm{d}T}{\mathrm{d}t}. \tag{22}$$

(b)   On the expression for ice-crystal number

As indicated in the beginning of this section, Eq. (14) is solved to give the number density of ice particles.

From Eq. (14), following the same route as Kärcher and Lohmann (2002a), we have a balance of terms driving the change in S:

$$\frac{a_1 S_{\mathrm{cr}}}{a_2 + a_3 S_{\mathrm{cr}}}w = R_{\mathrm{i}}, \tag{23}$$

where w is the vertical velocity of an adiabatic air parcel, and the coefficients a_1, a_2, and a_3 (which depend on temperature, T, and air pressure, p) are given by Kärcher and Lohmann (2002a) and are defined in the list of nomenclature in appendix B. S_{cr} is an approximation of saturation maximum, having applied Eq. (13). R_{i}, the number of water molecules consumed by the depositional growth of all ice particles in a unit volume per unit time, is an integral. When the size distribution of aerosols is taken into consideration, R_{i} is integrated down from a sufficiently large particle size to determine the radius of the smallest aerosol particles that freeze, r_{s}, achieved when R_{i} accumulates to balance the left-hand side of Eq. (23). Then, the number density of ice particles is given by integrating through the aerosol particles larger than r_{s}.

In the integral of R_{i}, a complementary error function appears. Asymptotic expansions for erfc(x) are available for $x \gg 1$ or for $x \ll 1$. These cases have been discussed by Kärcher and Lohmann (2002b). However, most homogeneous nucleation events take place in the upper troposphere under the conditions of κ close to 1, as can be seen from Fig. 1 of Kärcher and Lohmann (2002b). Unfortunately, both asymptotic expansions for $x \gg 1$ and for $x \ll 1$ are divergent when x is close to 1. Here, we give a fit to erfc(x) as

$$\exp\left(\frac{1}{\kappa}\right)\sqrt{\pi}\,\mathrm{erfc}\left(\sqrt{\frac{1}{\kappa}}\right) \approx \frac{3}{2\sqrt{\frac{1}{\kappa}} + \sqrt{\frac{1}{\kappa} + \frac{9}{\pi}}}, \tag{24}$$

which produces errors within 0.7%, verified by series expansions (erfc is the complementary error function). The mathematics describing the water-vapour consumption term with the above fit is detailed in appendix A.
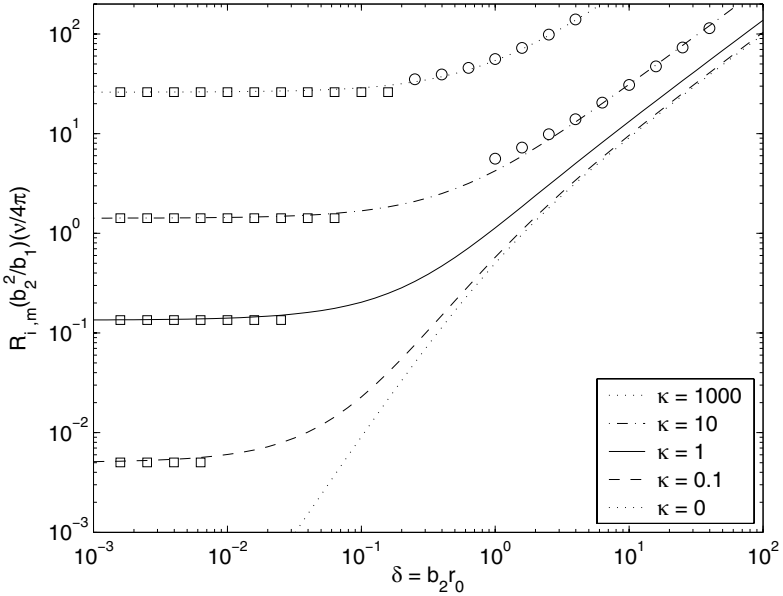
Figure 2.   The normalized monodisperse freezing/growth term, $R_{\mathrm{i,m}}(b_2^2/b_1)(v/4\pi)$, (see text) as a function of aerosol size, δ, for different constant freezing timescales, κ. Limiting cases in applicable conditions are indicated by circles (Eq. (A.10)), the lower dotted line (Eq. (A.11)), and squares (Eq. (A.13)).

The number density of ice particles at cloud formation is moderately sensitive to aerosol sizes. The normalized freezing/growth integral for monodisperse aerosols, a dimensionless quantity, $R_{\mathrm{i,m}}(b_2^2/b_1)(v/4\pi)$, is shown in Fig. 2 as a function of δ with constant κ. It is clear that the size of aerosols has an effect on the number of ice particles formed by homogeneous nucleation, unless the aerosol particles are small enough that δ can be taken as 0. This is the limiting case (A.13), shown by squares in Fig. 2. The critical value of δ, when (A.13) becomes applicable, depends on κ. The bigger κ is, the bigger the critical value of δ. This is shown clearly by the squares in Fig. 2. Further, suppose $\delta \ll 1$; Eq. (A.10) predicts no size dependence, while (A.11) predicts a second-order size dependence (through δ). The size effect increases from none to the second-order dependence with decreasing nucleation timescale τ (i.e. $\kappa \propto \tau$). For $\delta \gg 1$, both (A.10) and (A.11), together with (A.12), predict a first-order size dependence. Therefore, for $\kappa \gg 1$, the size effect increases from none to first-order dependence with increasing δ. For example, as $\kappa = 1000$ is big enough to use the limiting case of (A.10) (see the upper row of circles in Fig. 2), size dependence is present for $\delta > 0.1$ (aerosol sizes larger than $0.1/b_2$). For $\kappa \ll 1$ with increasing δ, the size effect increases from none to second-order, then decreases, finally to first-order. So, as stated above, the number of ice particles formed is independent of the aerosol size only when the aerosol particles are so small that $\delta \to 0$. Contrary to the discussion of Kärcher and Lohmann (2002a,b), there is not a separation between a fast-growth regime and a slow-growth regime that can be clearly indicated by $\kappa = 1$.

(c)   *For monodisperse aerosol particles*

Calculating (A.9), determining r_s by (A.5), then integrating (A.7) to get the number density of ice particles is not a completely analytical method, since (A.5) and (A.7) are

integral equations. However, for monodisperse aerosol particles, r_0 becomes a single-value parameter instead of a variable that describes the aerosol size spectrum, so there is no integration with respect to r_0, and there is no need to use Eq. (A.4). From (A.5), using the same approximation as Kärcher and Lohmann (2002b), the number density of ice particles is achieved directly by

$$n_i = \frac{S_{cr}}{S_{cr} - 1} \frac{a_1 w}{\left\{ R_{i,m}(r_0) \frac{b_2^2}{b_1} \frac{v}{4\pi} \right\} \frac{4\pi D}{b_2}} \leqslant n_a, \tag{25}$$

since a_2 exceeds $a_3 S_{cr}$ by at least a factor of three, as indicated by Kärcher and Lohmann (2002a). Equation (25) is kept in this form because the expression within the braces is the normalized freezing/growth integral for monodisperse aerosol (a dimensionless quantity, shown in Fig. 2), which may be replaced by any expression between braces from Eqs. (A.9) to (A.13). For $\kappa \gg 1$, inserting any of (A.12), (A.13), or (A.10) into (25) produces a relation $n_i \propto w^{3/2}$ (since $\kappa \propto \tau \propto 1/w$). For $\kappa \ll 1$, when aerosol particles are rather big, combining (25) with (A.12) gives $n_i \propto w$; when aerosol particles are rather small, $n_i \propto w^2$ is a coarse approximation from (25) with (A.13), while Kärcher and Lohmann (2002b) obtained $n_i \propto w^3$ with a second-order-accurate expansion of erfc(x). We have compromized to achieve a universal expression. In any case, the number density of ice particles can always be achieved by combining (25) with (A.9), as shown in Fig. 3. Although monodisperse aerosol particles are used, we get number densities of ice particles that are even closer than Kärcher and Lohmann (2002a,b) to the number densities of the detailed model. Evidence of improvement is that there is no crossing of lines for different aerosol sizes at the highest vertical velocities for 200 K and 220 K. Equation (25), together with (A.9), can be easily combined into general-circulation models (GCMs) to simulate cirrus clouds formed from aqueous aerosol particles. It also provides a way to check if a fully dynamical/microphysical cirrus model with homogeneous nucleation is coded correctly by providing an analytical test case (cf. Lin *et al.* 2002). Above all, an analytical expression has the merit that physical relationships are described definitely. For example,the dependence of n_i on the deposition coefficient α can be singled out. α is included in both b_1 and b_2, and hence in δ and κ. The dependence is $n_i \propto 1/R_{i,m}(\alpha)$, through the growth rate of ice particles, different for each limiting case (see (A.10)–(A.13)). The relationship given here is clearer than the numerical test results of Lin *et al.* (2002). However, Eq. (25) is not perfect. If the range of vertical velocities in Fig. 3 is extended to 20 m s^{-1}, the levelling off in the upper right corner, as in Fig. 4 of Kärcher and Lohmann (2002b), will appear. This, as a limitation of the parametrization, is discussed in the next section.

(d)   Limitation

The total volume of aqueous aerosols is not constant in a cloud-formation event. This is the defect in the parametrization. Figure 3 plots the ice number concentration, n_i, against updraught velocity, w, for various temperatures. The parametrization returns constant values for large w at low temperatures (not shown in Fig. 3, i.e. for $w > 10$ m s^{-1}), as in the upper right corner of Fig. 4 of Kärcher and Lohmann (2002b). In this section, we give an explanation for this levelling off of the parametrizations. The discrepancies between parametrization and detailed model result from the omission of the second term in the right-hand side of (18), d$\{\ln V(t)\}/$dt, which Eq. (A.3) guarantees to be zero in the parametrization. In fact, the total volume of aqueous aerosols does change during a nucleation event, so d$\{\ln V(t)\}/$dt cannot be zero. When the updraught
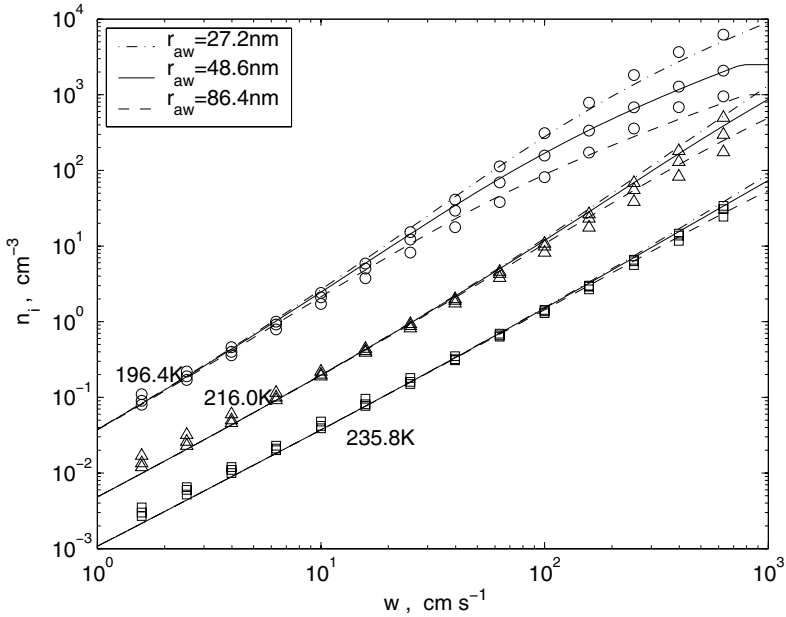
Figure 3. The number density of ice particles, n_i, as a function of the vertical velocity, w, for three freezing temperatures. The surface-area-weighted radii, r_{aw}, used as the monodisperse aerosol for the parametrization, are indicated in the key. The wet size at the freezing thresholds, 235.8 K, 216.0 K, and 196.4 K are magnified by factors of 7.2, 2.4, and 2.1, respectively, as demonstrated by Kärcher and Lohmann (2002b). The circles, triangles, and squares are microphysical model results provided by Kärcher and Lohmann.

velocity is high at lower temperatures, nearly all the available aqueous aerosols freeze. Given the same homogeneous nucleation rate coefficient, $V(t)$ changes faster for larger aerosol sizes. In this case, the omitted term is negative and the nucleation timescale is underestimated, so the ice number is overestimated, even up to the upper bound imposed by the total number of aerosols at which the ice number levels off. The inverse of the timescale, τ^{-1}, arrived at from (18), can be negative, meaning that the nucleation rate decreases with time, i.e. that part of the nucleation event after the peak in the nucleation rate. The parametrization discussed here neglects this part of the nucleation event because of the technical difficulty in dealing with a time-dependent τ. The error incurred can be compensated for by the choice of critical saturation S_{cr}. In this sense it is, perhaps, more useful to regard S_{cr} as an adjustable parameter whose value is indicated, but not fixed, by Eq. (10). The role of S_{cr} in directly determining the number of ice crystals is clearly shown by (25), i.e. the number is proportional to $S_{cr}/(S_{cr} - 1)$. Considering that nucleation takes place at saturation around S_{cr}, another indirect, but more significant, role of S_{cr} is through its effect on the nucleation timescale, τ. The relationship between J and Δa_w given by Koop *et al.* (2000) dictates a maximum c in Eq. (20) at $\Delta a_w = 0.3076$, so Eq. (10) (which gives $\Delta a_w = 0.3063$) is almost the best to make τ in (18) as big as possible.

On the other hand, this limitation of the parametrization is seldom reached under real atmospheric conditions, at least at the resolution of meteorological analyses (e.g. ERA-40*). The range of the normalized freezing/growth integral for monodisperse

* The 40-year reanalysis performed by the European Centre for Medium-Range Weather Forecasts.

aerosols in Fig. 2 is determined as the part $0.01 < \delta < 10$ and $0.01 < \kappa < 1000$. There is no single limiting case suitable for these ranges of δ and κ.

4.   NUCLEATION WITH ICE NUCLEI PRESENT

The atmosphere is not clear of solid aerosols. Soot (DeMott *et al.* 1999) and mineral dusts (Zuberi *et al.* 2002) can serve as ice nuclei. This section addresses how ice nuclei modify cirrus clouds. Section 4(a) gives conditions under which ice nuclei suppress homogeneous nucleation. When such conditions are not satisfied, homogeneous nucleation will take place to generate secondary ice particles, the number density of which is calculated in section 4(b), with an example in section 4(c).

(a)   Suppressed homogeneous-nucleation conditions

The condition that homogeneous nucleation doesn't take place is given by inequality (11), which is very simple in format, but not so straightforward to use since we do not yet have a solution for S_{max}. This difficulty can be circumvented with the help of the imaginary case (9).

The maximum of saturation is given by

$$\frac{dS}{dt}\bigg|_{S=S_{max}} = 0. \tag{26}$$

The solution to (26), considering (5), is

$$S_{max} = \frac{\tau_g^{-1}(t_{max})}{\tau_g^{-1}(t_{max}) - \tau_u^{-1}}. \tag{27}$$

Substituting (27) in (11) leads to

$$\tau_g^{-1}(t_{max}) > \frac{S_{cr}}{S_{cr} - 1}\tau_u^{-1}. \tag{28}$$

This inequality describes the relationship between the two timescales at the time of maximum saturation ratio. The problem is that we don't know either S_{max} or t_{max}. To make practical use of inequality (28), the imaginary case, in which the depositional growth of ice particles doesn't assume water vapour (given by Eq. (9) and shown by the dotted line in Fig. 1), is used. Then

$$t_{cr} = \tau_u \ln\left(\frac{S_{cr}}{S_0}\right) \tag{29}$$

is the time for an air parcel with a constant thermodynamical timescale to reach the homogeneous-nucleation saturation-ratio threshold. This imaginary case sets up an upper limit for the evolution of saturation as

$$S(t) \leq S_u(t). \tag{30}$$

When $t_{max} < t_{cr}$, i.e. the time, t_{max}, to reach the saturation-ratio maximum is shorter than the time, t_{cr}, to reach the homogeneous-nucleation threshold in the 'updraught-controlled' limit,

$$\{S_{max} = S(t_{max})\} \leq S_u(t_{max}) < \{S_u(t_{cr}) = S_{cr}\}, \tag{31}$$

the inequality (11) is satisfied automatically, and the cloud evolves through heterogeneous nucleation and growth only.

When conditions are such that $t_{max} \geq t_{cr}$, inequality (28) is guaranteed by

$$\tau_g^{-1}(t_{cr}) > \frac{S_{cr}}{S_{cr} - 1}\tau_u^{-1}, \tag{32}$$

because

$$\tau_g^{-1}(t_{max}) \geq \tau_g^{-1}(t_{cr}). \tag{33}$$

In the imaginary case, the growth of cloud particles can be given, according to Kärcher and Lohmann (2002b), as

$$\frac{dr_u}{dt} = \frac{b(S_u - 1)}{1 + b_2 r_u}, \tag{34}$$

with the initial condition

$$r_u(0) = r_i(0) = r_0, \tag{35}$$

where $b(S_u - 1)$ is b_1.

Integrating (34) and (35) gives

$$r_u(t_{cr}) = \frac{\sqrt{(1 + b_2 r_0)^2 + 2bb_2\tau_u[S_{cr} - S_0 - \ln(S_{cr}/S_0)]} - 1}{b_2}. \tag{36}$$

This imaginary case also sets up an upper limit for the size of ice particles as

$$r_i(t) \leq r_u(t). \tag{37}$$

When (3), (32) and (37) are used to determine the number density of ice nuclei,

$$\left\{ N = \frac{\tau_g^{-1}(t_{cr})}{4\pi D r_i(t_{cr})} \right\} > \frac{\tau_u^{-1}}{4\pi D r_i(t_{cr})} \frac{S_{cr}}{S_{cr} - 1}$$

$$\geq \left\{ \frac{\tau_u^{-1}}{4\pi D r_u(t_{cr})} \frac{S_{cr}}{S_{cr} - 1} = N_{C1} \right\}. \tag{38}$$

Inequality (32) is a sufficient condition for ice nuclei to suppress homogeneous nucleation. However, the condition (38) is compromised by the use of $r_u(t_{cr})$ rather than realistic ice-particle sizes $r_i(t_{cr})$. N_{C1} is the lowest number of ice nuclei that the theory assures us can prevent homogeneous nucleation in an 'updraught-controlled' cloud.

There is another upper limit for the size of ice particles that can be achieved by assuming all the water is in the condensed phase, so

$$r_i(t) < r_\infty = \left(\frac{3S_0 e_{s,i}}{4\pi N R_v T \rho_i} \right)^{1/3}. \tag{39}$$

When (3), (28) and (39) are used to determine the number density of ice nuclei,

$$N = \frac{\tau_g^{-1}(t_{max})}{4\pi D r_i(t_{max})} > \frac{\tau_u^{-1}}{4\pi D r_\infty} \frac{S_{cr}}{S_{cr} - 1}, \tag{40}$$

and the number density can be expressed as a function of thermodynamic conditions (including S_0) and updraught velocity, by substituting for τ_u^{-1}, r_∞ and D:

$$N > \frac{5.4 \times 10^{10} w^{1.5} p^{1.5}}{T^{5.41}(S_0 e_{s,i})^{0.5}} \left(\frac{S_{cr}}{S_{cr} - 1} \right)^{1.5} = N_{C2}. \tag{41}$$
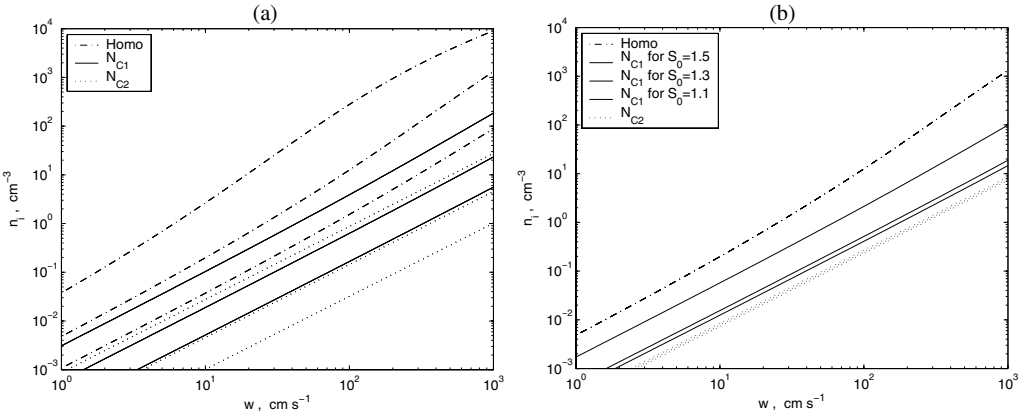
Figure 4.   (a) The number density of ice particles, n_i, formed by homogeneous nucleation (dash-dotted lines), N_{C1} (solid lines), and N_{C2} (dotted lines), as a function of the vertical velocity, w, for three freezing temperatures (196.4 K, 216.0 K, and 235.8 K—from top to bottom for each quantity). (b) The critical values of n_i for N_{C1} (solid lines) and N_{C2} (dotted lines) as a function of the vertical velocity, w, for three initial saturation ratios S_0 at which heterogeneous nucleation takes place. The temperature is 216 K. Also shown is the number density of ice crystals by homogeneous nucleation (dash-dotted line).

Inequality (41) is a necessary condition in that (39) must be satisfied in any circumstances. Equation (41) resembles (21) of Gierens (2003) in several aspects, principally because the diffusivity of water vapour in air has been given the same way.

The dependence of N_{C1} and N_{C2} on w and T, and on w and S_0, is shown in Figs. 4(a) and (b), respectively. Note that the lines for N_{C1} and N_{C2} do not cross and N_{C1} is always greater than N_{C2} for the same conditions, as we would expect. To the accuracy we can achieve, given our assumptions, condition (38) is a sufficient condition, and condition (41) is a necessary condition, for the suppression of homogeneous nucleation. There must be a critical value, N_C, between N_{C2} and N_{C1}, for which

$$N > N_C \qquad (42)$$

is a sufficient and necessary condition. If condition (42) is satisfied (which implies that condition (41) must be satisfied, but condition (38) might not be), homogeneous nucleation will be suppressed by existing ice particles produced by heterogeneous nucleation.

The role of ice nuclei in determining the number density of ice particles is shown schematically in Fig. 5. With increasing number density of ice nuclei, the number density of ice particles produced by a cloud formation event first decreases to some point where homogeneous nucleation is just suppressed, then increases linearly with ice nuclei. In other words, the presence of ice nuclei can either decrease or increase the number density of ice particles in a cirrus cloud; but before homogeneous nucleation is completely suppressed, the number density of ice particles must be lower than when there is pure homogeneous nucleation. This analysis provides a framework for, amongst other things, the interpretation of model results. For example, the comparisons of HN-ONLY runs (homogeneous nucleation only) and ALL-MODE simulations (both heterogeneous and homogeneous nucleation allowed) by Lin *et al.* (2002) can, therefore, be clarified by Fig. 5.
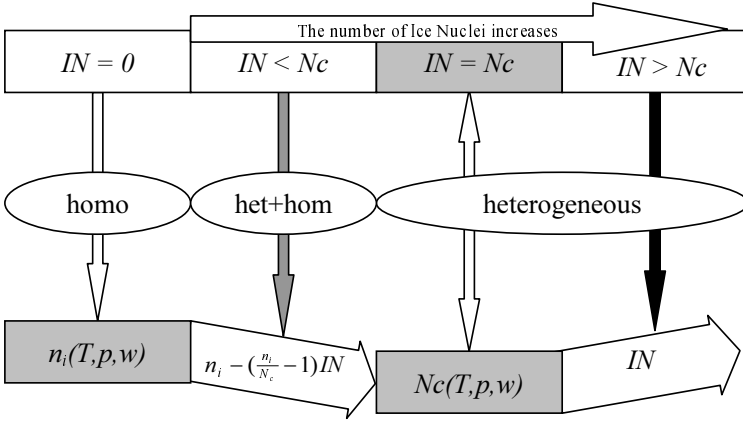
Figure 5.   Schematic of the determination of the number density of ice particles in a cirrus cloud that has been newly formed by freezing aerosol droplets. The number density of ice nuclei is shown in the top row, the nucleation regimes in the middle row, the number of ice particles in the bottom row. Vertical arrows represent controls. Dark arrows mean strong control, hollow arrows means weak control, and the grey one means complex. Notations: IN = the number density of ice nuclei; n_i = the number density of ice particles formed by homogeneous nucleation; Nc = the critical number density for ice nuclei.

(b)   Secondary homogeneous nucleation

When the number density of ice nuclei is smaller than the critical value N_c, uptake of water vapour onto ice particles activated from them is insufficient to prevent the supersaturation ratio from reaching the critical value for homogeneous nucleation. In such cases, this consumption of water vapour by existing ice particles, as well as the number of ice particles, n_i', formed by homogeneous nucleation, must also be taken into account when calculating R_i. R_i defined by (A.1) now includes an additional term, $N(4\pi/v)r_u^2(t_{cr})\,dr_u/dt$, contributed by ice particles previously activated by heterogeneous nucleation, as does the right-hand side of Eq. (A.5). Using the monodisperse aerosol example, the balance at the peak of the saturation ratio is

$$\frac{a_1 S_{cr}}{a_2 + a_3 S_{cr}} w = n_i' R_{i,m}(r_0) + N \frac{4\pi}{v} r_u^2(t_{cr}) \frac{dr_u}{dt}, \tag{43}$$

where n_i' is the number density of additional ice particles generated by secondary homogeneous nucleation, and N is the number density of ice particles previously activated by heterogeneous nucleation.

Assuming $b_2 r_u(t_{cr}) \gg 1$ to simplify (34), together with the approximation used in (25), we have

$$n_i' = n_i - \frac{b_2 r_u(t_{cr})}{\left\{ R_{i,m}(r_0) \frac{b_2^2}{b_1} \frac{v}{4\pi} \right\}} N. \tag{44}$$

Equation (44) clearly shows that, up to a certain limit, increasing the number density of ice nuclei will decrease the number density of ice particles. We call the multiplier to N in (44) the *homogeneous-nucleation depression efficiency*. Figure 6(a) and (b) show this efficiency as a function of updraught velocities, temperatures, and the saturation ratios, S_0, at which ice nuclei activate. Figure 6 shows that one ice nucleus can prevent the formation of up to 100 homogeneously-formed cirrus particles per unit volume. This effect is strongest for high updraught velocities, low temperatures, and low ice-nuclei-activation supersaturations, S_0. For different S_0, the efficiency can differ by up to an
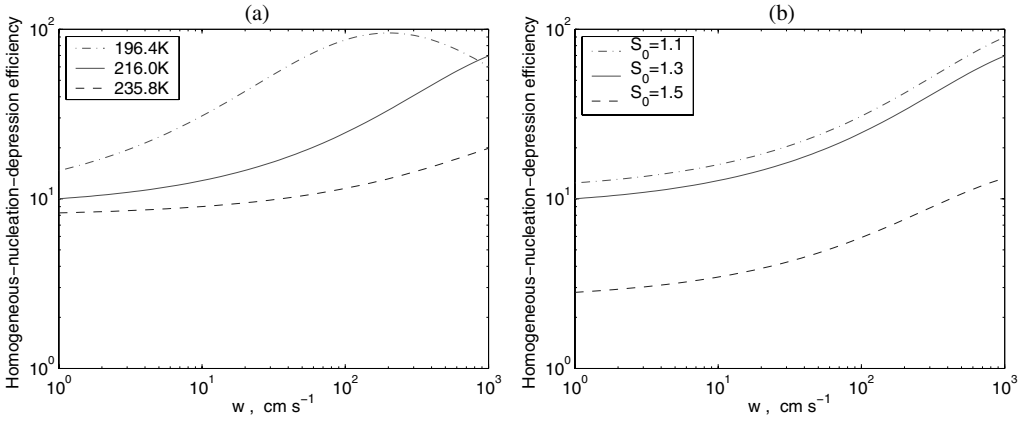
Figure 6. (a) The efficiency of an ice-nucleus-depressing homogeneous nucleation as a function of temperature and updraught. $S_0 = 1.3$. (b) The efficiency of an ice-nucleus-depressing homogeneous nucleation as a function of updraught and S_0 at $T = 216.0$ K. The saturation mixing ratio S_0 at which the ice nucleus activates is the parameter in the model that encapsulates the chemical composition of the ice nucleus.

order of magnitude. This demonstrates that different kinds of ice nuclei may radically affect the number density of ice particles. The nonlinear response of the efficiency to S_0 means that it is more important to quantify the total number of ice nuclei with S_0 less than a moderate value (1.3, say) than to define precisely the spectrum of activities between 1.0 and 1.3 for these nuclei.

The physical requirement $n_i' \geq 0$ for (44) leads to

$$N \leq N_C = N_{C1}. \tag{45}$$

This is the prerequisite to use (44). It's not surprising that we find again that N_{C1} is the critical value separating the nucleation regimes, since equivalent approximations have been used. Numerical tests show that the error incurred by using N_{C1} for N_C is of the same order as uncertainties in water-vapour diffusivity. To the accuracy of the current theory, Eq. (44) can be rewritten as

$$n_i' = n_i \left(1 - \frac{N}{N_{C1}}\right). \tag{46}$$

The sum of n_i' and N is the number density of ice particles generated by hybrid nucleation, shown in Fig. 5. If, somehow, $r_i(t_{max})$ is known, then a better result can be achieved by using $\sum_j N_j r_{i,j}(t_{max})$ in (44) accordingly, which is the effect of existing ice particles, no matter whether they are generated by heterogeneous nucleation or are left from a former cloud event. In practice, we can directly calculate n_i' before determining whether the prerequisite (45) is satisfied or not. A negative value of n_i' indicates that homogeneous nucleation is suppressed.

(c) *The size distribution generated by hybrid nucleation*

Bi-modal size distributions of ice particles are common (Ivanova *et al.* 2001; Donovan and Lammeren 2002). This phenomenon can be attributed—at least in part—to secondary homogeneous nucleation. Figure 7 shows size spectra from 26 September 1997 in the outflow from Hurricane Nora (Ivanova *et al.* 2001). We use this as a test case to demonstrate use of our cirrus parametrizations. The main features of the observed size
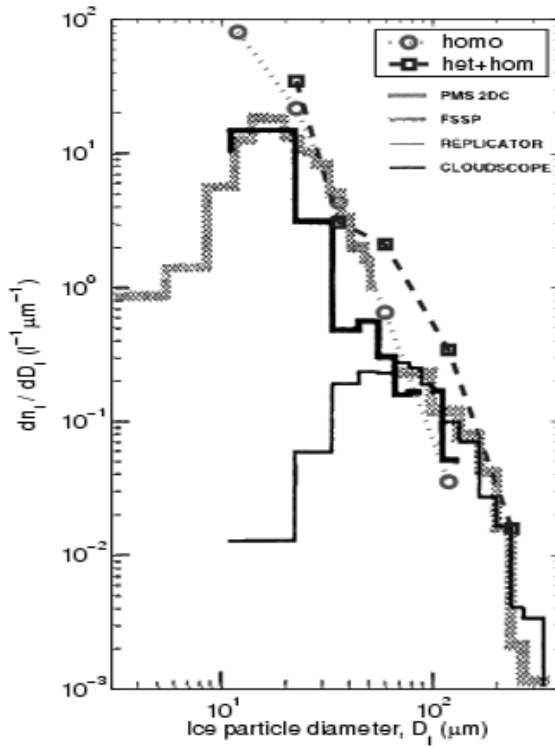
Figure 7. Size spectra on 26 September 1997 for the DOE–ARM Intensive Observing Period in the Hurricane Nora outflow at 1909:15–1911:00 UTC, for temperatures −48.3 to −50.3 °C, and pressures 216.53 to 209.12 hPa. The size distributions reconstructed by parametrizations are imposed by squares joined by the dashed line (including heterogeneous nucleation) and circles joined by the dotted line (without heterogeneous nucleation). Reprinted from *Atmos. Res.* **59–60,** Ivanova *et al.*, 'A GCM parameterization for bimodal size spectra and ice mass removal rates in mid-latitude cirrus clouds', 89–113, Copyright (2001) with permission from Elsevier.

spectra are captured by the parametrization including heterogeneous nucleation using a simple average of eight calculations (squares in Fig. 7). The calculations are done at −49.2 °C and 220 hPa, with an adiabatic cooling rate of 0.0094 °C m^{-1}. The updraughts we use are 0.02, 0.04, 0.08, 0.16, 0.32, 0.64, and 1.2 m s^{-1}, respectively. Given the activated ice nuclei as a function of supersaturation (Meyers *et al.* 1992; Pruppacher and Klett 1997),

$$N = \exp\{-0.639 + 0.1296(S - 100)\} - 0.5278 \qquad (47)$$

per litre. A correction term has been added to make the value zero at just-saturated conditions. We find secondary homogeneous nucleation takes place when the updraught is greater than 1 m s^{-1}. The size distribution is reconstructed from various sizes of ice particle using the parametrization developed in section 4(b). To do this, Eq. (47) is sectioned as in Table 1. The size of secondary homogeneously-nucleated ice particles is estimated by

$$n'_\text{i}\rho_\text{i}\frac{4\pi}{3}r_\text{i}^3 + \sum_j N_j\rho_\text{i}\frac{4\pi}{3}(r_{u,j} + \Delta_j)^3 = \frac{(S_\text{cr} - 1)e_{\text{s, i}}}{R_\text{v}T}, \qquad (48)$$

which keeps the conservation of mass at equilibrium. Δ_j is an adjustment so that heterogeneously nucleated ice particles are never smaller than homogeneously nucleated

TABLE 1. ASSUMED NUMBER DENSITIES OF ICE NUCLEI ACCORDING TO EQ. (47)

Section range of S	1.0–1.1	1.1–1.3	1.3–1.4	1.4–1.45	1.45–1.48
Number density (l^{-1})	1.40	23.8	68.4	85.9	100
Activation S_0	1.0	1.1	1.3	1.4	1.45

ice particles. Also shown in Fig. 7 is the size distribution by the parametrization without heterogeneous nucleation (circles in Fig. 7), otherwise the conditions are same. Comparing with the observations, although the agreement is not quantitatively precise, it evidently demonstrates that (secondary) homogeneous nucleation produces the dominant mode of smaller size (about 15 μm diameter). On the other hand, a few bigger ice particles are from ice nuclei (or existing ice particles).

The example is shown here only to demonstrate that hybrid nucleation can generate bi-modal size distributions of ice particles. There is no further information to convince us that we have assumed the proper ice-nuclei distribution. There are also other processes (say, aggregation) which can also generate a bi-modal size distribution.

5. SUMMARY AND CONCLUSIONS

In the upper troposphere, ice crystals form by aerosol freezing, either homogeneously or heterogeneously (or both), in supersaturated conditions. Homogeneous nucleation takes place only when saturation is above a critical value. Nucleation regimes, i.e. either heterogeneous-dominant or homogeneous-dominant freezing, can be differentiated by comparing virtual supersaturation mixing ratios with the critical supersaturation mixing ratio required by homogeneous nucleation. The introduction of an imaginary case—particle growth without vapour depletion—untangles the interaction between the supersaturation change and the growth of ice crystals.

An existing parametrization of homogeneous nucleation has been improved by using a theoretically determined timescale of homogeneous freezing, and has been made practicable by providing a universal analytical expression. The improved parametrization works well, even when monodisperse aerosol particles are used in determining cirrus ice-crystal number densities, if the aerosol distribution can be described adequately by a single effective radius. The discrepancies between the parametrization and a detailed model—in cirrus ice-crystal number densities at lower temperatures and higher updraughts—are explained by the change of the nucleation timescale with respect to time.

The number densities of ice particles in cirrus clouds formed by heterogeneous freezing of aerosol particles are determined by the number density of ice nuclei contained in an ascending air parcel, provided that the nuclei density exceeds a critical value, N_{C1}. However, the critical value is dictated by the atmospheric conditions (specifically the temperature, T, and the updraught velocity, w) and the ice-nucleation properties of aerosol particles (i.e. the (super-)saturation at which the ice nuclei activate, S_0). If the number density of ice nuclei in an air parcel is lower than the critical value, homogeneous nucleation will take place to compensate for this deficit, so that the critical value is the minimum number of ice particles in a cirrus cloud formed from aerosol freezing.

The analytical solution of homogeneous nucleation provides a parametrization scheme for cirrus clouds in the upper troposphere. This nearly single-line parametrization merits potential applications in GCMs and climate models. On the other hand, confident modelling taking the role of ice nuclei into consideration awaits more

information on ice nuclei. Our analysis suggests that the critical information is the total number density of ice nuclei with low-to-moderate activation supersaturations, rather than details of the activation spectrum inside this supersaturation range, since all the low-to-moderate activating ice nuclei have similar efficiencies in depressing homogeneously nucleated ice-particle number densities. Nevertheless, the critical value provides a lower limit for the number density of ice particles in a cirrus cloud, and is helpful for understanding the role of ice nuclei in climate.

APPENDIX A

The water-vapour consumption term

This appendix gives the integral for water vapour consumed by all frozen aerosols, shows how the number density of ice particles is separated from the integral with two contradictory assumptions, and deduces the limiting cases.

The water-vapour consumption term in Eq. (23) is defined by

$$R_i = \frac{1}{\nu} \int_{r_s}^{\infty} \int_{-\infty}^{t} 4\pi r_i^2(r_0, t_0, t) \frac{dr_i}{dt}(r_0, t_0, t) \frac{d\dot{n}_i}{dr_0}(r_0, t_0) \, dt_0 \, dr_0, \qquad \text{(A.1)}$$

where ν is the specific volume of a water molecule in ice. The number density of ice particles can only be separated from R_i with two, contradictory, assumptions. Firstly, to remove the nucleation rate from (A.1), Eq. (15) is assumed applicable to each size-bin so that

$$\frac{dn_i}{dr_0}(r_0, t) = \int_{-\infty}^{t} \frac{d\dot{n}_i}{dr_0}(r_0, t_0) \, dt_0 = \frac{d\dot{n}_i}{dr_0}(r_0, t)\tau. \qquad \text{(A.2)}$$

The assumption used to get (A.2) is that τ for each size-bin is a constant. To ensure τ for each size-bin is a constant, from Eq. (18), we need

$$\frac{\partial}{\partial t_0} \left\{ \frac{dn_a}{dr_0}(r_0, t_0) \right\} = 0, \qquad \text{(A.3)}$$

where $(dn_a/dr_0)\Delta r_0$ is the number concentration of aerosol particles in a bin of size r_0.

Secondly, since larger aerosol particles have a higher probability of freezing, all particles larger than r_s are assumed to have been frozen at time t (although this is not allowed by (A.3)), then

$$\frac{dn_i}{dr_0}(r_0, t) = \frac{dn_a}{dr_0}(r_0, t_0 = -\infty), \qquad \text{(A.4)}$$

where $t_0 = -\infty$ means the time when the aerosol particles have swollen but no freezing has started. This assumption is later used to convert unknowns dn_i/dr_0 for each size-bin to one single unknown r_s. It can be avoided by assuming monodisperse aerosol particles, as given in section 3(c).

Applying (15) to (A.1), then combining it with (A.2) and (A.4) gives

$$R_i = \int_{r_s}^{\infty} R_{i,m}(r_0) \frac{dn_a}{dr_0}(r_0, t_0 = -\infty)\, dr_0, \qquad (A.5)$$

where the monodisperse (at radius of r_0) freezing/growth term is defined by

$$R_{i,m}(r_0) = \frac{4\pi}{v} \int_{-\infty}^{t} \frac{1}{\tau} \exp\left(-\frac{t - t_0}{\tau}\right) r_i^2(r_0, t_0, t) \frac{dr_i}{dt}(r_0, t_0, t)\, dt_0, \qquad (A.6)$$

and the integral limit r_s, in (A.5), is the only unknown. When Eq. (A.5) is solved for r_s by the method of Kärcher and Lohmann (2002b), the total number of ice crystals is given by

$$n_i = \int_{r_s}^{\infty} \frac{dn_a}{dr_0}(r_0, t_0 = -\infty)\, dr_0 \leq n_a. \qquad (A.7)$$

The monodisperse freezing/growth term, after integration, is

$$\begin{aligned}
R_{i,m}(r_0) = \frac{4\pi}{v} \frac{b_1}{b_2^2} &\left\{ \left(\frac{1+\delta}{2}\sqrt{\kappa} + \frac{1}{1+\delta}\frac{1}{\sqrt{\kappa}}\right) \right. \\
&\left. \times \exp\left(\frac{1}{\kappa}\right) \sqrt{\pi}\, \mathrm{erfc}\left(\frac{1}{\sqrt{\kappa}}\right) + \delta - 1 \right\},
\end{aligned} \qquad (A.8)$$

where b_1, b_2, δ, and κ follow the definitions given by Kärcher and Lohmann (2002b) and appendix B. Inserting (24) into (A.8) produces an equation with an analytical solution suitable for all cases, i.e.

$$\begin{aligned}
R_{i,m}(r_0) = \frac{4\pi}{v} \frac{b_1}{b_2^2} &\left\{ \frac{1+\delta}{2}\left(\frac{3\kappa}{2+\sqrt{1+\frac{9}{\pi}\kappa}}\right) \right. \\
&\left. + \frac{1}{1+\delta}\left(\frac{3}{2+\sqrt{1+\frac{9}{\pi}\kappa}}\right) + \delta - 1 \right\}.
\end{aligned} \qquad (A.9)$$

There are four limiting cases that can be deduced directly from the above all-case equation.

When $\kappa \to \infty$, (A.9) becomes

$$R_{i,m}(r_0)|_{\kappa \to \infty} = \frac{4\pi}{v} \frac{b_1}{b_2^2}\left(\frac{1+\delta}{2}\sqrt{\pi\kappa}\right) = \frac{1}{v}\left(2\pi\frac{b_1}{b_2}\right)^{3/2}\sqrt{\tau}, \qquad (A.10)$$

which is (13a) and (13b) of Kärcher and Lohmann (2002b).

When $\kappa \to 0$, (A.9) becomes

$$R_{i,m}(r_0)|_{\kappa \to 0} = \frac{4\pi}{v} \frac{b_1}{b_2^2}\left(\frac{\delta^2}{1+\delta}\right), \qquad (A.11)$$

which is Eq. (15c) of Kärcher and Lohmann (2002b).

When $\delta \to \infty$, (A.9) becomes

$$R_{i,m}(r_0)|_{\delta \to \infty} = \frac{4\pi}{v} \frac{b_1}{b_2^2}\left\{\frac{\delta}{2}\left(\frac{3\kappa}{2+\sqrt{1+\frac{9}{\pi}\kappa}}\right) + \delta\right\}, \qquad (A.12)$$

which is superior to Eq. (15b) of Kärcher and Lohmann (2002b) in that it is always valid, even when κ is big.

When $\delta \to 0$, (A.9) becomes

$$R_{i,m}(r_0)|_{\delta \to 0} = \frac{4\pi}{\nu} \frac{b_1}{b_2^2} \left(\frac{\frac{3}{2}\kappa + 3}{2 + \sqrt{1 + \frac{9}{\pi}\kappa}} - 1 \right), \qquad (A.13)$$

which is superior to Eq. (15a) of Kärcher and Lohmann (2002b) as it is always valid, no matter what value κ is.

APPENDIX B

Notation

a_k, b_k coefficients defined as

$$a_1 = \frac{L_s g}{c_p R_v T^2} - \frac{g}{R_d T}$$

$$a_2 = \frac{M_w R_v T}{N_a e_{s,i}}$$

$$a_3 = \frac{\varepsilon M_w L_s^2}{N_a c_p p T}$$

$$b = \frac{\alpha}{\rho_i} \frac{e_{s,i}}{\sqrt{2\pi R_v T}}$$

$$b_1 = b(S - 1)$$

$$b_2 = \frac{\alpha}{D} \sqrt{\frac{R_v T}{2\pi}}$$

C freezing timescale coefficient
D diffusivity of water molecules in air
δ $= b_2 r_0$, dimensionless aerosol radius
Δa_w excess of water activity
e water-vapour pressure
$e_{s,i}$ saturation water-vapour pressure over ice
J homogeneous-nucleation rate coefficient

κ $= \dfrac{2b_1 b_2 \tau}{(1 + \delta)^2}$ dimensionless freezing timescale

L_s latent heat of water sublimation
n_a (total) number density of aerosol particles
n_i (total) number density of ice particles
n_i' number density of additional ice particles generated by secondary homogeneous nucleation
$\dot{n}_i$ nucleation rate
N number density of ice nuclei
N_C critical value for the number density of ice nuclei
ν specific volume of a water molecule in ice

p	air pressure
r_0	aerosol radius or ice-particle radius at time t_0
r_i	ice-particle radius
r_u	time-dependent upper limit for ice-particle radius
r_s	radius of the smallest aerosol particles that freeze
r_∞	absolute upper limit for ice-particle radius
R_d	gas constant of air
R_i	depositing rate of number density of water molecules
$R_{i,m}$	monodisperse freezing/growth integral
R_v	gas constant of water vapour
ρ_i	mass density of ice
S	saturation ratio
S_0	saturation ratio at which ice nuclei activate
S_{cr}	saturation ratio above which significant homogeneous freezing takes place
S_{max}	the highest saturation ratio an ascending air-parcel experiences
S_u	updraught-only controlled saturation
t	time (usually at present tense, at which R_i is calculated)
t_0	time (usually at past tense, at which particles freeze)
t_{max}	time when saturation is at peak
t_{cr}	time required for an updraught to increase saturation from S_0 to S_{cr}
T	temperature
τ	freezing timescale
τ_g	depositional timescale for saturation change
τ_u	thermodynamical timescale for saturation change
V	total volume density of liquid aerosols
w	vertical velocity

REFERENCES

DeMott, P. J., Rogers, D. C. and Kreidenweis, S. M. 1997 The susceptibility of ice formation in upper tropospheric clouds to insoluble components. *J. Geophys. Res.*, **102,** 19575–19584

DeMott, P. J., Chen, Y., Kreidenweis, S. M., Rogers, D. C. and Sherman, D. E. 1999 Ice formation by black carbon particles. *Geophys. Res. Lett.*, **26,** 2429–2432

Donovan, D. P. and van Lammeren, A. C. A. P. 2002 First ice cloud effective particle size parameterisation base on combined lidar and radar data. *Geophys. Res. Lett.*, **29,** doi: 10.1029/2001GL013731

Ford, I. 1998 How aircraft nucleate ice particles: A simple model. *J. Aerosol Sci.*, **29,** S1117

Gierens, K. 2003 On the transition between heterogeneous and homogeneous freezing. *Atmos. Chem. Phys.*, **3,** 437–446

IPCC 2001 *Climate change 2001: The scientific basis. Third assessment report*. Eds. Sir John Houghton and Yihui Ding, Cambridge University Press, New York

Ivanova, D., Mitchell, D. L., Arnott, W. P. and Poellot, M. 2001 A GCM parameterization for bimodal size spectra and ice mass removal rates in mid-latitude cirrus clouds. *Atmos. Res.*, **59–60,** 89–113

Kärcher, B. and Lohmann, U. 2002a A parameterization of cirrus cloud formation: Homogeneous freezing of supercooled aerosols. *J. Geophys. Res.*, **107**(D2)**,** 4010, doi: 10.1029/2001JD000470

2002b A parameterization of cirrus cloud formation: Homogeneous freezing including effects of aerosol size. *J. Geophys. Res.*, **107**(D23)**,** 4698, doi: 10.1029/2001JD001429

2003 A parameterization of cirrus cloud formation: Heterogeneous freezing. *J. Geophys. Res.*, **108**(D14)**,** 4402, doi: 10.1029/2002JD003185

Koop, T., Luo, B. P., Tsias, A. and Peter, T.   2000   Water activity as the determinant for homogeneous ice nucleation in aqueous solution. *Nature*, **406,** 611–614

Lin, R.-F., Starr, D. O'C., DeMott, P. J., Cotton, R., Sassen, K., Jensen, E., Kärcher, B. and Liu, X.   2002   Cirrus parcel model comparison project. Phase 1: The critical components to simulate cirrus initiation explicitly. *J. Atmos. Sci.*, **59**(15)**,** 2305–2329

Lynch, D. K.   1996   Cirrus clouds: Their role in climate and global change. *Acta Astronautic*, **38,** 859–863

Meyers, P. J., DeMott, P. J. and Cotton, W. R.   1992   New primary ice-nucleation parameterisations in an explicit cloud model. *J. Appl. Meteorol.*, **31,** 708–721

Pruppacher, H. R. and Klett, J. D.   1997   *Microphysics of clouds and precipitation.* Kluwer Academic Publishers, Norwell, Mass., USA

Santacesaria, V., Carla, R., MacKenzie, R., Adriani, A., Cairo, F., Didonfrancesco, G., Kiemle, C., Redaelli, G., Beuermann, J., Schiller, C., Peter, T., Luo, B., Wernli, H., Ravegnani, F., Ulanovsky, A., Yushkov, V., Sitnikov, N., Balestri, S. and Stefanutti, L.   2003   Clouds at the tropical tropopause: A case study during the APE-THESEO campaign over the western Indian Ocean. *J. Geophys. Res.*, **108**(D2)**,** 4044, doi: 10.1029/2002JD002166

Sassen, K. and Benson, S.   2000   Ice nucleation in cirrus clouds: A model study of the homogeneous and heterogenous modes. *Geophys. Res. Lett.*, **27**(4)**,** 521–524

Zhang, Y., Macke, A. and Alers, F.   1999   Effect of crystal size spectrum and crystal shape on stratiform cirrus radiative forcing. *Atmos. Res.*, **52,** 59–75

Zuberic, B., Bertram, A. K., Cassa, C. A., Molina, L. T. and Molina, M. J.   2002   Heterogeneous nucleation of ice in $(NH_4)_2SO_4$–H_2O particles with mineral dust immersions. *Geophys. Res. Lett.*, **29**(10)**,** doi: 10.1029/2001GL014289